ARCHIVES
of
FOUNDRY ENGINEERING

ISSN (2299-2944)
Volume 2026
Issue 1/2026

27 – 34

3/1

10.24425/afe.2026.157966

Published quarterly as the organ of the Foundry Commission of the Polish Academy of Sciences

Investigation of Electrochemical Behaviour Related to the Microstructures of Different Aluminium Alloys Used in the Automotive Industry

Eda Ergün Songül
Istanbul University-Cerrahpasa, Faculty of Engineering, Metallurgical and Materials Engineering Department, Turkey
Corresponding author: E-mail address: eda.ergunsongul@iuc.edu.tr

Received 25.09.2025; accepted in revised form 19.12.2025; available online 27.02.2026

Abstract

Aluminium casting alloys are extensively used in the automotive sector, with Al–Si–Cu systems such as A380 favoured for their excellent castability and cost-effectiveness. In contrast, Al–Cu based alloys like A206 provide superior mechanical strength but are often regarded as less corrosion resistant, restricting their use in aggressive environments. Despite their industrial relevance, a direct comparative assessment of these alloys under controlled solidification conditions remains scarce.
In this study, the electrochemical behaviour of Al–5Cu (A206) and Al–8Si–3Cu (A380) alloys were systematically investigated as a function of microstructure, modified through sand and permanent mould casting. Potentiodynamic polarization tests were performed in 3.5 wt.% NaCl solution to evaluate corrosion potential (E_{corr} vs. Ag/AgCl) and current density (I_{corr}). Microstructural characterization revealed significant dendrite refinement and reduced secondary dendrite arm spacing (SDAS) in permanent mould castings compared with sand castings. Although A380 exhibited finer SDAS than A206, its corrosion resistance was consistently inferior due to the galvanic activity between eutectic Si and Al_2Cu phases. By contrast, the simpler binary microstructure of A206 limited cathodic heterogeneity, allowing refinement to translate into improved electrochemical stability.
The results demonstrate that corrosion resistance in aluminium casting alloys is governed not only by microstructural parameters but also by alloy chemical composition. These findings extend current understanding of the microstructure–corrosion relationship and provide practical guidance for alloy selection in automotive applications. A206 alloy, when cast under optimized conditions, emerges as a promising candidate for structural components exposed to chloride-rich service environments.

Keywords: Aluminium casting alloys, Corrosion, Microstructure, A206, A380

1. Introduction

Aluminium casting alloys are extensively applied in the transportation and aerospace industries owing to their high strength-to-weight ratio, ease of manufacturability, and good corrosion resistance under moderate conditions. Among them, Al–Si-based alloys are the most prevalent in automotive applications because of their excellent castability, cost-effectiveness, and wear resistance imparted by eutectic silicon [1–3]. In contrast, Al–Cu alloys such as A206 provide tensile strengths exceeding 450 MPa, which makes them attractive for aerospace components where mechanical performance is critical

[4]. However, their comparatively lower corrosion resistance has traditionally restricted their application in aggressive service environments [5–7]. High-strength aerospace casting alloys and quality factor assessments have long highlighted the trade-offs between alloy chemistry, microstructure, and performance [8]. Comparative studies of aerospace aluminium alloys have similarly underscored the balance between strength and corrosion sensitivity in Al–Cu systems [9].

The corrosion performance of aluminium alloys is determined by a combination of alloy chemistry, solidification conditions, microstructural features (e.g., dendrite size, secondary dendrite arm spacing—SDAS), and the type and distribution of intermetallic phases [10–12]. In Al–Si–Cu systems, copper-rich phases such as Al_2Cu generate electrochemical microcells that promote localized corrosion [13], while eutectic silicon networks act as cathodic sites, accelerating anodic dissolution of the α-Al matrix [14]. Refinement of SDAS through higher cooling rates is known to improve corrosion resistance by homogenizing phase distribution and reducing galvanic interactions [15]. Recent reviews have reinforced this conclusion, underscoring the decisive role of SDAS and intermetallic morphology in governing corrosion susceptibility in cast aluminium alloys [16].

Several recent studies have demonstrated that solidification-induced heterogeneities strongly influence corrosion susceptibility [16-18]. In these works, permanent mould casting (or analogous higher cooling rate conditions) generally provides improved corrosion resistance compared to sand casting, due to finer microstructures and more uniform phase distributions [16-18]. Alloy modification, particularly Sr addition, has been shown to refine eutectic morphologies and improve the performance of Al–Si–Cu alloys [4]. However, excessive Cu content may still promote galvanic corrosion, underscoring the complex role of alloy chemistry. Collectively, these findings confirm that microstructural engineering offers a viable pathway for optimizing corrosion behaviour in aluminium casting alloys.

Despite the industrial relevance of A206 and A380 alloys, systematic comparative studies on their corrosion performance under controlled casting conditions remain limited. A380 is widely adopted in automotive components because of its excellent fluidity and cost-efficiency, yet its high Si content and multiphase microstructure often reduce corrosion resistance. A206, on the other hand, offers higher strength and simpler phase morphology but requires heat treatment and has traditionally been regarded as less corrosion resistant [4, 19]. The absence of direct comparative data under equivalent solidification conditions represents a gap in current knowledge.

In this context, the present study aims to evaluate and contrast the electrochemical behaviour of Al–5Cu (A206) and Al–8Si–3Cu (A380) alloys processed through sand and permanent mould casting. By correlating corrosion parameters namely corrosion potential (E_{corr}) and current density (I_{corr}) with secondary dendrite arm spacing and interdendritic phase distribution, this work provides new insights into the interplay between alloy composition, microstructure, and corrosion response. The outcomes are expected to inform alloy selection and casting strategies for automotive and structural components exposed to chloride-rich environments.

2. Materials and Methods

2.1. Alloy Composition and Casting Procedure

Two commercially available aluminium casting alloys, Al–5Cu (A206) based and Al–8Si–3Cu based (A380), were selected because of their widespread use in structural and automotive applications. The nominal chemical compositions listed in Table 1 were obtained from the manufacturer's certificate and were not experimentally re-analysed in this study.

Table 1.
Nominal chemical compositions of A206 and A380 aluminium casting alloys (wt.%)

	Fe	Si	Cu	Mn	Mg	Ti	Al
A206	0.107	0.328	4.75	0.394	0.161	0.245	balance
A380	0.13	7.75	2.65	0.01	0.27	0.13	balance

Each alloy was cast using two different moulding techniques: sand mould and permanent mould casting. The objective was to generate distinct microstructural variations between the two moulding conditions. Melting was carried out in a resistance furnace under identical processing conditions. The A206 alloy was melted at 730 ± 5 °C, while A380 was melted at 710 ± 5 °C. Cylindrical specimens with a diameter of 10 mm and a height of 120 mm were produced.

For permanent mould casting, steel moulds were preheated to 200 °C to minimize thermal shock and to promote directional solidification. The sand mould was not preheated and remained at ambient laboratory temperature prior to casting. Although solidification time was not directly measured, the thermal conditions employed in this study align well with established solidification profiles reported for sand and permanent mould castings of comparable aluminium alloy systems. No heat treatment was applied; all specimens were examined in the as-cast condition to ensure that the effects of solidification-induced microstructural features—particularly SDAS—could be isolated without the influence of post-processing thermal modifications. Previous studies have shown that higher mould preheating refines SDAS and promotes a more homogeneous phase distribution.

2.2. Microstructural Characterization

The solidified specimens were sectioned, ground, and polished using standard metallographic techniques. Optical microscopy (OM) was employed to observe the microstructures, and images were obtained using an inverted metallurgical microscope at various magnifications (5× and 10×).

Secondary dendrite arm spacing (SDAS) was measured manually from the micrographs using ImageJ software. The linear intercept method was applied, whereby the distance between adjacent secondary arms was measured across multiple randomly selected fields of view. This approach allowed a comparative analysis of grain refinement across different casting methods.

Dendrite size was quantified using the linear-intercept method on polished optical micrographs, providing an independent assessment of overall dendritic morphology in addition to SDAS.

2.3. Electrochemical Testing

The corrosion behaviour of the samples was investigated by potentiodynamic polarization testing in a 3.5 wt.% NaCl aqueous solution at room temperature (23 ± 1 ºC). Prior to testing, the specimen surfaces were ground using 1200-grit SiC paper, rinsed with ethanol, and dried with compressed air. A three-electrode electrochemical cell configuration was used, with the aluminium specimen as the working electrode, a silver/silver chloride electrode (Ag/AgCl) as the reference, and platinum as the counter electrode. The exposed surface area of the samples was maintained at 1 cm².

Open circuit potential (OCP) was monitored for 30 minutes to ensure system stabilization. Potentiodynamic scans were then conducted from –200 mV to +500 mV relative to OCP at a scan rate of 1 mV/s. Corrosion current density (I_{corr}) and corrosion potential (E_{corr}) values were determined by Tafel extrapolation using the Gamry Echem Analyst software.

3. Results

3.1. Microstructural Observations

Figure 1 and Figure 2 present the optical micrographs of A206 and A380 alloys cast via permanent and sand moulds. The measured secondary dendrite arm spacing (SDAS) was approximately 25 µm in permanent mould castings and about 80 µm in sand castings for A206, whereas the corresponding values for A380 were around 17 µm and 30 µm, respectively. For clarity, reproducibility, and measurement accuracy, the SDAS values were quantified directly on the corresponding microstructural regions using ImageJ software. Prior to analysis, each micrograph was calibrated using the embedded scale bar to convert pixel dimensions into micrometers, and contrast optimization (brightness/threshold adjustment) was applied to enhance dendrite arm definition. The line-intercept method was then used along the traces illustrated in Figure 2(b), which represent the actual measurement paths employed during the quantitative assessment.

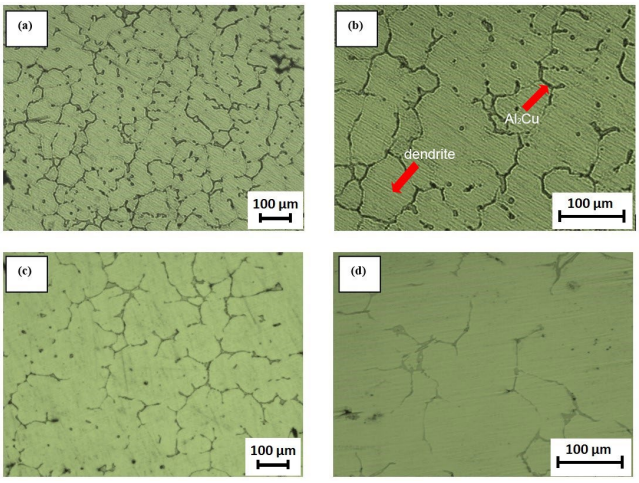

Fig. 1. Optical micrographs of A206 alloy cast under different moulding and magnification conditions: (a) permanent mould – 5×, (b) permanent mould – 10×, (c) sand mould – 5×, (d) sand mould – 10×

The eutectic phase in A206 was primarily composed of Al_2Cu, whereas A380 exhibited a multiphase structure dominated by eutectic Si. The volume fraction of interdendritic phases increased under slower cooling in sand cast samples for both alloys. These results agree with previous studies indicating that lower cooling rates promote coarsening and segregation of secondary constituents in aluminium casting alloys [1,2]. Permanent mould castings exhibited finer dendritic structures due to enhanced cooling, while sand mould castings produced coarser grains and more pronounced interdendritic segregation (Figure 1 and 2).

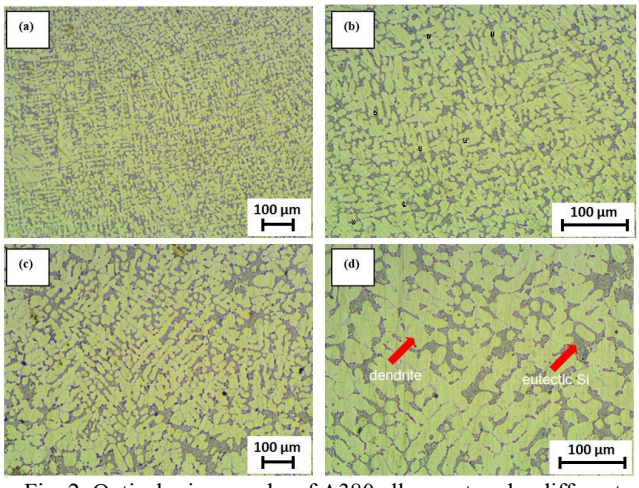

Fig. 2. Optical micrographs of A380 alloy cast under different moulding and magnification conditions: (a) permanent mould – 5×, (b) permanent mould – 10×, (c) sand mould – 5×, (d) sand mould – 10×

3.2. Dendrite Size Comparison

Figure 3 compares the dendrite sizes of A206 and A380 alloys under different moulding conditions. In both alloys, permanent mould castings produced finer grain structures owing to higher cooling rates. A206 samples consistently exhibited larger grains than A380 under identical processing parameters. This behaviour can be attributed to the wider liquidus–solidus temperature interval and lower Si content of A206, both of which limit nucleation and grain refinement. Conversely, the high Si content in Al–Si–Cu systems enhances nucleation and results in finer grain structures [3,4].

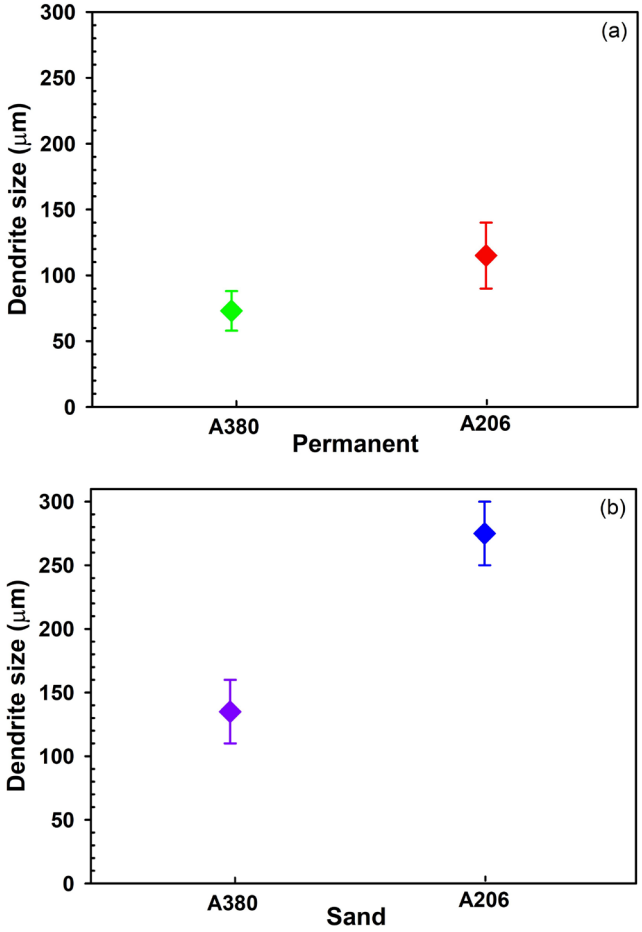

Fig. 3. Dendrite size comparison of A206 and A380 aluminium alloys under permanent (a) and sand (b) mould casting conditions

3.3. Electrochemical Behaviour: Individual Alloy Analysis

Potentiodynamic polarization curves for A206 and A380 alloys cast via sand and permanent moulds in 3.5 wt.% NaCl solution are shown in Figures 4 and 5. In both alloys, I_{corr} values were relatively close between the two casting methods, but E_{corr} values were consistently more positive in the permanent mould castings, indicating improved corrosion resistance. This observation is consistent with prior studies showing that refined microstructures can reduce galvanic microcell formation and promote more stable passive films [5,6].

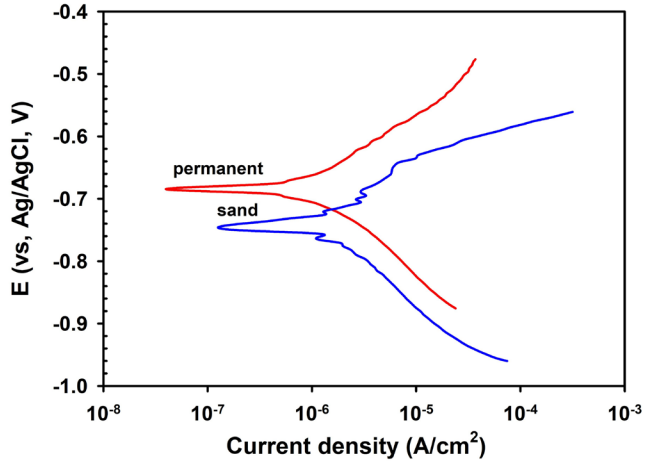

Fig. 4. Potentiodynamic polarization curves of A206 alloy cast using sand and permanent moulds in 3.5 wt.% NaCl solution

For A206, E_{corr} improved from –0.75 V (sand mould) to –0.68 V (permanent mould) (vs. Ag/AgCl). For A380, E_{corr} shifted from –0.62 V (sand mould) to –0.58 V (permanent mould) (vs. Ag/AgCl). Although A380 exhibited finer SDAS, its higher eutectic Si and Cu content promoted localized electrochemical activity and reduced overall corrosion resistance. Eutectic Si networks act as cathodic sites and exacerbate galvanic corrosion when heterogeneously distributed [14].

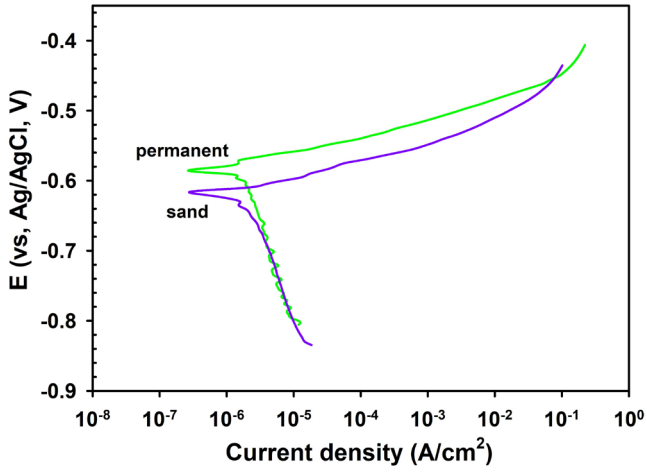

Fig. 5. Potentiodynamic polarization curves of A380 alloy cast using sand and permanent moulds in 3.5 wt.% NaCl solution

3.4. Comparative Analysis: A206 vs. A380

Figures 6 and 7 compare the polarization curves of A206 and A380 alloys under identical casting conditions. A206 consistently

demonstrated lower I_{corr} values, reflecting superior corrosion performance. In contrast, A380 displayed more noble E_{corr} values but higher I_{corr}, indicating that its apparent thermodynamic advantage did not translate into better corrosion resistance. This behaviour reflects the influence of alloy chemistry: the simpler binary microstructure of A206 limits cathodic heterogeneity and favours lower dissolution rates, whereas the multiphase constitution of A380 comprising eutectic Si, Al_2Cu, and Fe-rich phases promotes galvanic interactions that accelerate corrosion [13,14,16].

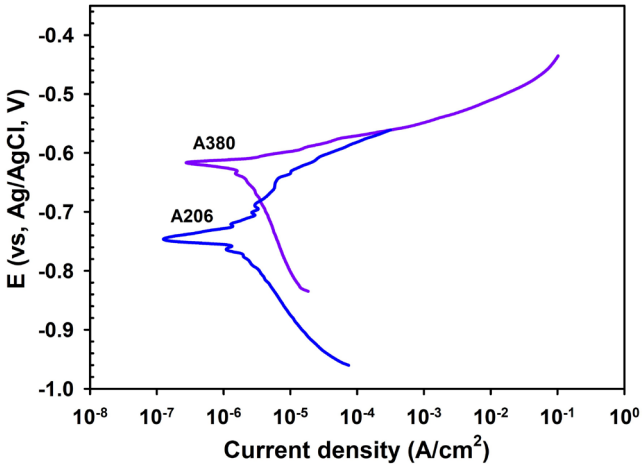

Fig. 6. Tafel polarization curves of A206 and A380 alloys cast using sand moulds in 3.5 wt.% NaCl solution

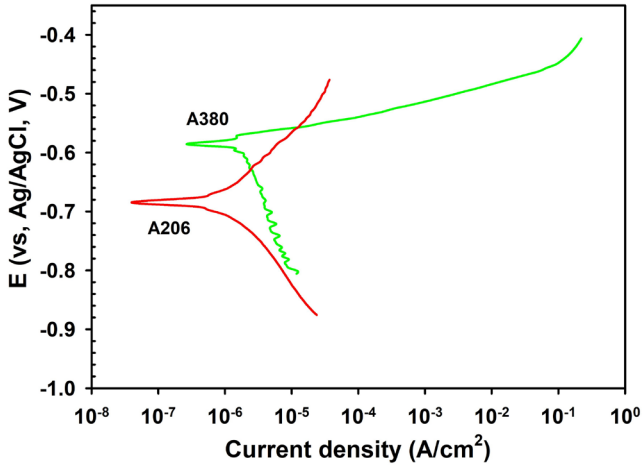

Fig. 7. Tafel polarization curves of A206 and A380 alloys cast using permanent moulds in 3.5 wt.% NaCl solution

Figure 8 summarises I_{corr} of A206 and A380 aluminium alloys for the two moulding routes in 3.5 wt.% NaCl. For each alloy, the permanent mould condition yields I_{corr} values that are lower than those of the corresponding sand mould condition, consistent with the refinement-driven mitigation of anodic kinetics. When the two alloys are compared under the same casting route, A206 systematically exhibits lower I_{corr} than A380, evidencing a reduced tendency for localised dissolution in the Al–Cu system within the present testing window. The separation between alloys is most apparent under the sand mould condition, where microstructural heterogeneity in A380 translates into a higher I_{corr}. Overall, the trends in Figure 8 align with the microstructural evidence (finer SDAS and a more uniform interdendritic phase distribution in permanent mould castings) and support the conclusion that casting route modulates corrosion rate primarily through its influence on microstructural heterogeneity.

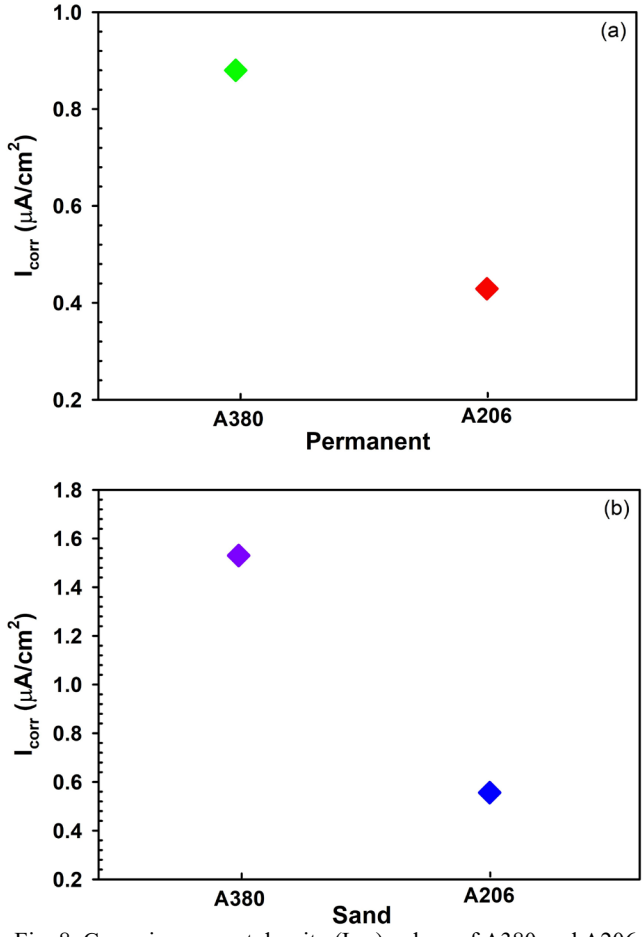

Fig. 8. Corrosion current density (I_{corr}) values of A380 and A206 aluminium alloys obtained by (a) permanent mould casting and (b) sand mould casting, evaluated in 3.5 wt.% NaCl solution

Figure 9 presents the corrosion potential (E_{corr}) values of the A206 and A380 aluminium alloys under permanent and sand mould conditions in 3.5 wt.% NaCl. In both alloys, permanent mould castings exhibit more positive E_{corr} values than their sand mould counterparts, indicating a beneficial effect of microstructural refinement on passivity. When the two alloys are compared under the same casting route, A380 consistently shows nobler E_{corr} values than A206, reflecting the influence of its multiphase microstructure on corrosion potential. However, this apparent thermodynamic advantage does not translate into superior corrosion resistance, as corroborated by the higher I_{corr} values of A380. The difference between the alloys is most pronounced in the sand mould condition, where heterogeneous phase distribution in A380 leads to a marked shift towards more

positive E_{corr} without a corresponding reduction in corrosion rate. These findings emphasise that E_{corr} trends must be interpreted together with current density data to provide a complete assessment of electrochemical stability.

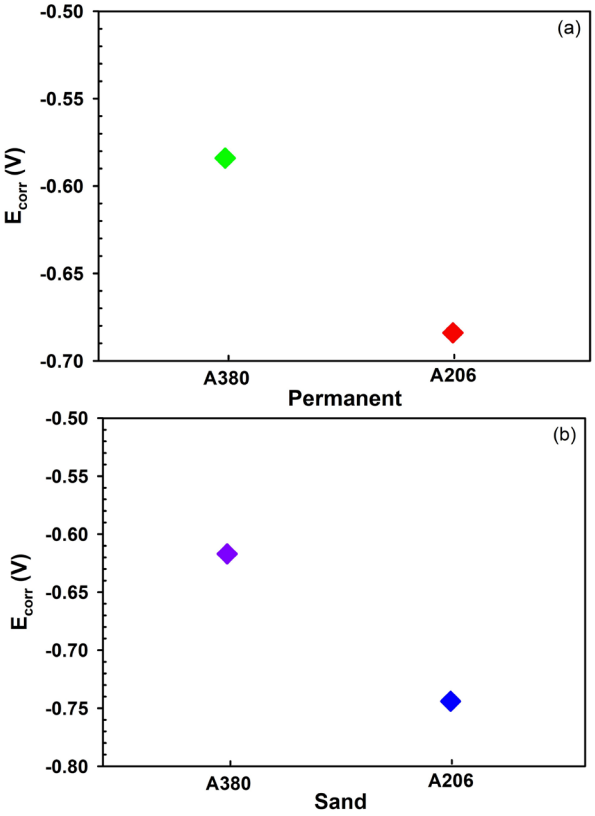

Fig. 9. Corrosion potential (E_{corr}) values of A380 and A206 aluminium alloys obtained by (a) permanent mould casting and (b) sand mould casting, evaluated in 3.5 wt.% NaCl solution

Furthermore, while SDAS plays a role in governing corrosion behaviour, its effect is alloy-dependent. In A206, grain refinement correlated with improved corrosion resistance, whereas in A380 the effect was overshadowed by the electrochemical activity of eutectic constituents. These findings confirm that microstructural morphology must be evaluated in conjunction with phase chemistry when predicting corrosion performance [4,14].

3.5. Correlation Between Microstructure and Corrosion Resistance

Figure 10 illustrates the relationship between dendrite size and electrochemical corrosion parameters (I_{corr} and E_{corr}) for A206 and A380 alloys. A near-linear correlation is observed in A206, where smaller grains and finer SDAS lead to lower I_{corr} and more positive E_{corr} values. In contrast, the correlation in A380 is less pronounced due to the dominant role of eutectic Si in determining corrosion response. This alloy-specific behaviour highlights the interplay between microstructural refinement and electrochemical heterogeneity. The influence of eutectic silicon in particular has been well-documented in recent studies, which emphasize its function as a cathodic phase accelerating matrix dissolution under chloride exposure [14,16]. These microstructure–corrosion correlations are further elaborated in Section 4 to highlight alloy-specific mechanisms governing the electrochemical behaviour of A206 and A380.

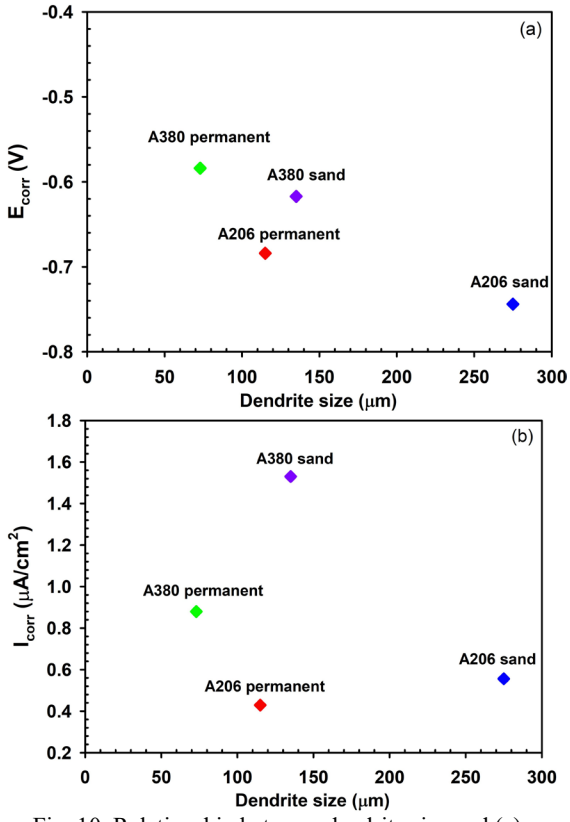

Fig. 10. Relationship between dendrite size and (a) corrosion potential (E_{corr}) and (b) corrosion current density (I_{corr}) of A380 and A206 aluminium alloys produced by permanent mould and sand mould casting in 3.5 wt.% NaCl solution

4. Discussion

The corrosion behaviour of A206 and A380 alloys was strongly dependent on both alloy composition and casting conditions. Sand mould castings generally produced coarser dendritic structures and larger SDAS, while permanent mould castings promoted microstructural refinement, yielding narrower dendritic arms and more uniform phase distributions. These variations were directly reflected in the electrochemical response, with permanent mould samples exhibiting more positive E_{corr} values (vs. Ag/AgCl) and lower I_{corr} values. Comparable behaviour has been reported in previous studies, where refined microstructures enhanced corrosion resistance by limiting galvanic coupling and stabilising passive films [16,18,20,21,22].

4.1. A206 Alloy

In A206, the microstructure was primarily characterized by the Al_2Cu phase. Sand mould castings exhibited a coarser structure (SDAS ≈ 80 μm), whereas permanent mould castings produced refined dendrites with narrower SDAS (≈ 25 μm). This refinement led to a clear improvement in corrosion behaviour, as reflected by a positive shift in E_{corr} and a reduction in I_{corr}. These results support earlier findings that faster solidification enhances corrosion resistance by producing a more homogeneous phase distribution [16,18]

Although Al_2Cu can act as a cathodic constituent and promote localized corrosion, its homogeneous distribution in permanent mould castings limited galvanic interactions, thereby improving corrosion resistance [1,13,14]. Nanoparticle modification has been shown to enhance the corrosion performance of A206 through microstructural refinement [12]. Recent alloy design studies also confirm that minor additions of transition elements such as Mn or Cr can refine intermetallic morphology and further stabilise corrosion resistance [23]. While the literature frequently categorizes A206 as mechanically strong but corrosion-prone, the present results demonstrate that controlled solidification can significantly improve its corrosion resistance [5,15,24]. Our results suggest that with controlled solidification, A206 can achieve significantly enhanced corrosion resistance, extending its potential applications.

4.2. A380 Alloy

The corrosion performance of A380 was dominated by its multiphase nature. Despite exhibiting finer SDAS values (17–30 μm) than A206, A380 consistently displayed inferior corrosion resistance. This outcome reflects the strong galvanic activity of eutectic Si and Al_2Cu, which overshadowed the beneficial effects of grain refinement. Similar findings have been reported, in which eutectic Si was identified as a dominant cathodic phase accelerating localized corrosion [14]. Furthermore, the presence of Fe-rich intermetallics, even in small amounts, has also been reported to contribute to localized attack [13].

Although modification strategies such as Sr addition have been shown to improve corrosion resistance in Al–Si–Cu alloys by refining eutectic morphologies, the unmodified A380 samples in this study confirmed the inherent susceptibility of such alloys to localized corrosion [3,4]. These results support the consensus that Al–Si–Cu alloys, while industrially advantageous in terms of castability, are intrinsically less corrosion resistant than Al–Cu alloys [14,16].

4.3. Comparative Analysis

A direct comparison of the two alloys confirmed that alloy chemistry exerts a more decisive influence on corrosion behaviour than SDAS alone. Both alloys benefitted from permanent mould casting, yet only A206 translated microstructural refinement into markedly improved corrosion resistance. In A380, the galvanic activity of eutectic Si and Al_2Cu phases dominated, regardless of dendrite size. The alloy-specific role of cathodic phases in governing corrosion susceptibility has also been emphasized in previous studies [3,14].

Interestingly, although A380 consistently exhibited finer SDAS than A206, its corrosion resistance was lower. This contradiction illustrates that SDAS cannot be treated as a universal predictor of corrosion behaviour, as phase chemistry can outweigh morphological refinement in determining electrochemical response [12].

The relationship between SDAS and corrosion behaviour was clearly alloy-dependent. In A206, refinement of the solidification structure likely reduced the effective α-Al/Al_2Cu galvanic intensity, enabling the finer interdendritic morphology to translate into improved corrosion performance. In contrast, the same refinement had a more limited impact in A380, where the electrochemical response is governed predominantly by the presence of eutectic Si, Al_2Cu and Fe-rich intermetallics [13,14]. These phases are well-known to act as strong cathodic sites in Al–Si–Cu systems, and their dominant influence can readily overshadow the beneficial effects expected from dendrite refinement alone [14].

Indeed, although A380 displayed more noble corrosion potentials (E_{corr}) than A206 under identical casting conditions, this trend did not coincide with lower corrosion rates, as reflected by its higher corrosion current densities (I_{corr}). A positive shift in E_{corr} primarily indicates the ease of passive film formation, but it does not prevent localized breakdown in multiphase alloys containing eutectic Si and Cu-rich intermetallics [13,14]. By contrast, I_{corr} directly quantifies dissolution rate and therefore provides a more reliable measure of corrosion severity [16]. Overall, the comparative results extend existing knowledge by showing that A206, when cast under optimized conditions, challenges its traditional classification as a mechanically strong but corrosion-sensitive alloy [15,24].

5. Conclusions

This study systematically compared the corrosion behaviour of Al–5Cu (A206) and Al–8Si–3Cu (A380) casting alloys as a function of microstructure, controlled through sand and permanent mould casting. Microstructural analysis confirmed that permanent mould casting consistently refined the dendritic network, yielding markedly smaller secondary dendrite arm spacing (SDAS) values in both alloys. Despite this refinement, A380 exhibited inferior corrosion resistance, primarily due to the galvanic activity of eutectic Si and Al_2Cu phases. In contrast, the simpler binary phase structure of A206 reduced cathodic heterogeneity, enabling microstructural refinement to translate more effectively into enhanced electrochemical stability. Electrochemical tests further showed that A206 consistently exhibited lower corrosion current densities (I_{corr}) than A380, while A380 displayed more noble corrosion potentials (E_{corr}) that did not correspond to superior corrosion resistance. This apparent discrepancy underscores the need to interpret E_{corr} and I_{corr} together when assessing alloy performance. Overall, the results demonstrate that corrosion behaviour in aluminium casting alloys is governed not only by the degree of microstructural refinement but also by the intrinsic electrochemical activity of constituent phases. From a practical perspective, A206, when produced under

controlled cooling conditions, emerges as a promising candidate for automotive and structural components exposed to chloride-rich environments. Future research should investigate the combined effects of microstructural control, alloy modification, and heat treatment strategies to further optimize the balance between strength and corrosion resistance.

References

[1] Zeren, M., Karakulak, E. & Gümüş, S. (2011). Influence of Cu addition on microstructure and hardness of near-eutectic Al-Si-xCu-alloys. *Transactions of Nonferrous Metals Society of China.* 21(8), 1698-1702. DOI: 10.1016/S1003-6326(11)60917-5.

[2] Basavakumar, K.G., Mukunda, P.G. & Chakraborty, M. (2007). Influence of grain refinement and modification on dry sliding wear behaviour of Al–7Si and Al–7Si–2.5Cu cast alloys. *Journal of Materials Processing Technology.* 186(1-3), 236-245. DOI: 10.1016/j.jmatprotec.2006.12.039.

[3] Wu, C.T., Lee, S.L., Hsieh, M.H. & Lin, J.C. (2010). Effects of Cu content on microstructure and mechanical properties of Al–14.5Si–0.5Mg alloy. *Materials Characterization.* 61(11), 1074-1079. DOI: 10.1016/j.matchar.2010.06.022.

[4] Shin, S.S., Kim, E.S., Yeom, G.Y. & Lee, J.C. (2012). Modification effect of Sr on the microstructures and mechanical properties of Al–10.5Si–2.0Cu recycled alloy for die casting. *Materials Science and Engineering: A.* 532, 151-157. DOI: 10.1016/j.msea.2011.10.076.

[5] Apelian, D. (2009). *Aluminium cast alloys: Enabling tools for improved performance.* Rosemont, IL: North American Die Casting Association.

[6] Ye, H. (2003). An overview of the development of Al-Si-alloy based material for engine applications. *Journal of Materials Engineering and Performance.* 12(3), 288-297. DOI: 10.1361/105994903770343132.

[7] Di Sabatino, M., Arnberg, L., Rørvik, S. & Prestmo, A. (2005). The influence of oxide inclusions on the fluidity of Al–7 wt.% Si alloy. *Materials Science and Engineering: A.* 413(1-2), 272-276. DOI: 10.1016/j.msea.2005.08.175.

[8] Din, T., Rashid, A.K.M.B. & Campbell, J. (1996). High strength aerospace casting alloys: Quality factor assessment. *Materials Science and Technology.* 12(3), 269-273. DOI: 10.1179/mst.1996.12.3.269.

[9] Din, T. & Campbell, J. (1996). High strength aerospace aluminium casting alloys: A comparative study. *Materials Science and Technology.* 12(8), 644-650. DOI: 10.1179/mst.1996.12.8.644.

[10] Ravi, K.R., Pillai, R.M., Amaranathan, K.R., Pai, B.C. & Chakraborty, M. (2008). Fluidity of aluminum alloys and composites: A review. *Journal of Alloys and Compounds.* 456(1-2), 201-210. DOI: 10.1016/j.jallcom.2007.02.038.

[11] Mohanty, P.S. & Gruzleski, J.E. (1995). Mechanism of grain refinement in aluminium. *Acta Metallurgica et Materialia,* 43(5), 2001-2012. DOI: 10.1016/0956-7151(94)00405-7.

[12] Pan, S., Yuan, J., Moodispaw, M.P., Linsley, C., Liu, J., Luo, A.A., Taub, A. & Li, X. (2022). Corrosion performance of nano-treated aluminum alloy A206 with TiC nanoparticles. *Materials and Corrosion.* 73(10), 419-429. DOI: 10.1002/maco.202213503.

[13] Liang, Z.X., Ye, B., Zhang, L., Wang, Q.G., Yang, W.Y. & Wang, Q.D. (2013). A new high-strength and corrosion-resistant Al–Si based casting alloy. *Materials Letters.* 97, 104–107. DOI: 10.1016/j.matlet.2013.01.112.

[14] Szklarska-Smialowska, Z. (1999). Pitting corrosion of aluminum. *Corrosion Science.* 41(9), 1743-1767. DOI: 10.1016/S0010-938X(99)00012-8.

[15] Sigworth, G.K. & DeHart, F. (2003). Recent developments in the high strength aluminium-copper casting alloy A206. *AFS Transactions.* 111(03-135), 341–354.

[16] Berlanga-Labari, C., Castro-Valdés, M., Grande, M.A., Cambronero, L.E.G. & Llorente, J.I. (2020). Corrosion of cast aluminum alloys: A review. *Metals.* 10(10), 1384, 1-29. DOI: 10.3390/met10101384.

[17] Cerdán Bernal, M.C. (2025). *Effect of microstructure on corrosion of cast aluminium alloys*. Unpublished master's thesis, Jönköping University, Jönköping, Sweden.

[18] Castro-Sastre, Á., Rodríguez, J., Velasco, R., Fernández, M., Camba, P. & Martínez, D. (2021). Comparative study on microstructure and corrosion resistance of Al–Si alloy cast from sand mold and binder jetting mold. *Metals.* 11(9), 1421, 1-16. DOI: 10.3390/met11091421.

[19] Tiryakioğlu, M., Campbell, J. & Alexopoulos, N.D. (2009). Quality indices for aluminum alloy castings: A critical review. *Metallurgical and Materials Transactions B.* 40(6), 802-811. DOI: 10.1007/s11663-009-9304-5.

[20] El Haj, B.A., Bouayad, A. & Alami, M. (2015). Effect of mould temperature and melt treatment on properties of an AlSi9 cast alloy: Thermal and microstructural investigations. *International Letters of Chemistry, Physics and Astronomy.* 55, 12-20. DOI: 10.56431/p-xzgx6e.

[21] Vandersluis, E. & Ravindran, C. (2017). Comparison of measurement methods for secondary dendrite arm spacing. *Metallography, Microstructure, and Analysis.* 6(1), 89-94. DOI: 10.1007/s13632-016-0331-8.

[22] Hu, X., Yan, H., Chen, W., Li, S. & Fu, H. (2011). Effect of sample diameter on primary and secondary dendrite arm spacings during directional solidification of Pb–26 wt.% Bi hypo-peritectic alloy. *Rare Metals.* 30(4), 424-431. DOI: 10.1007/s12598-011-0408-0.

[23] Qian, D., Lan, K. & Yang, Y. (2024). Microstructure evolution of a novel low-silicon cast aluminum alloy modified with Mn and Cr during solution treatment. *Materials Characterization.* 217, 114319, 1-13. DOI: 10.1016/j.matchar.2024.114319.

[24] Major, J.F. & Sigworth, G.K. (2006). Chemistry/property relationships in AA206 alloys. *AFS Transactions.* 114(06-029), 1–9.